Structure–Activity Relationships for Hypervalent Iodine Electrocatalysis

Brandon L. Frey
Phong Thai
Lauv Patel
David C. Powers*

Texas A&M University Department of Chemistry, 3255 TAMU, College Station TX 77843, USA
powers@chem.tamu.edu

Published as part of the
Special Issue Electrochemical Organic Synthesis

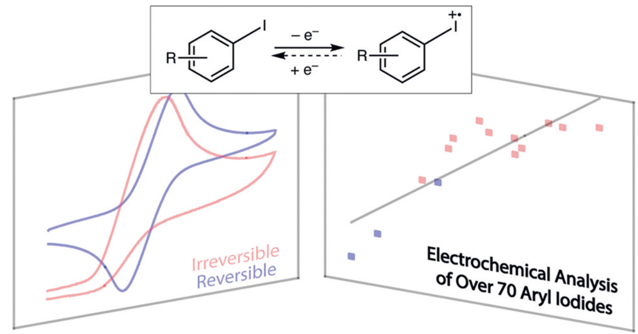

Received: 18.01.2023
Accepted: 06.02.2023
Published online: 06.02.2023 Accepted Manuscript), 16.03.2023 (Version of Record)
DOI: 10.1055/a-2029-0617; Art ID: SS-2023-01-0023-OP

Abstract The design and optimization of novel electrocatalysts requires robust structure–activity data to correlate catalyst structure with electrochemical behavior. Aryl iodides have been gaining attention as metal-free electrocatalysts but experimental data are available for only a limited set of structures. Herein we report electrochemical data for a family of 70 aryl iodides. Half-peak potentials are utilized as proxies for reduction potentials and reveal that, despite differences in electrochemical reversibility, the potential for one-electron oxidation of 4-substituted aryl iodides to the corresponding iodanyl radicals is well-correlated with standard Hammett parameters. Additional data are presented for 3- and 2-substituted aryl iodides, including structures with potentially chelating 2-substituents that are commonly encountered in hypervalent iodine reagents. Finally, potential decomposition processes relevant to the (in)stability of iodanyl radicals are presented. We anticipate that the collected data will advance the design and application of aryl iodide electrocatalysis.

Key words hypervalent iodine, electrochemistry, linear free-energy relationships, sustainable catalysis, oxidation

Aryl iodide electrocatalysis provides a conceptual platform to combine the inherent sustainability of electrochemical oxidation with the mechanistic diversity available to hypervalent iodine-mediated transformations.[1–5] Thus far, realization of this ideal has been plagued by challenges including 1) achieving selectivity for the oxidation of aryl iodides over the oxidatively labile nucleophiles needed for specific transformations, 2) developing strategies to aggregate multiple one-electron events to achieve the multielectron transformations that characterize synthetic organic chemistry, and 3) needing high applied potentials owing to the instability of odd-electron oxidation states (i.e., iodanyl radicals).[6–10] As a result, the application of aryl iodide electrochemistry is often limited to ex-cell applications in which anodic aryl iodide oxidation is temporally separated from substrate functionalization, which prevents undesired side reactions but obviates the potential for electrocatalysis.[11–16]

4-Iodoanisole has often been employed as the aryl iodide mediator in synthetic hypervalent iodine electrocatalysis because the electron-donating methoxy group suppresses the onset potential needed for anodic oxidation relative to iodobenzene.[6,17] Guided by the hypothesis that cooperative I–I redox could stabilize open-shell intermediates generated during anodic oxidation, we recently demonstrated one-electron anodic oxidation of aryl iodides to form isolable iodanyl radicals (i.e., I(II) species).[17,18] We further showed that these iodanyl radicals can promote mild and selective C–H/E–H coupling without necessitating two-electron iodine-centered oxidation. Although this discovery represented an advance in catalyst lifetime and turnover number, systematic studies to evaluate design principles in aryl iodide electrocatalysis were not pursued.

The lack of electrochemical data for a broad family of aryl iodides prevents systematic identification and optimization of this class of electrocatalysts. Herein, we report systematic studies of the structure–function relationships that dictate aryl iodide electrochemistry. Half-peak potentials, which are derived from cyclic voltammetry,[19] of 70 aryl iodides are collected. Below we present the results of these investigations organized by aryl iodide structure as follows: 1) 4-Substituted aryl iodides, 2) 2- and 3-substituted aryl iodides, 3) 2-substituted 4-iodoanisole derivatives, 4) 2-substituted iodoveratrole derivatives, and 5) additional miscellaneous electron-rich aryl iodides. After presenting these data, we discuss the potential decomposition mechanisms available to iodanyl radical intermediates that must be considered when designing new aryl iodide electrocatalysts.

Downloaded by: Texas A&M University. Copyrighted material.

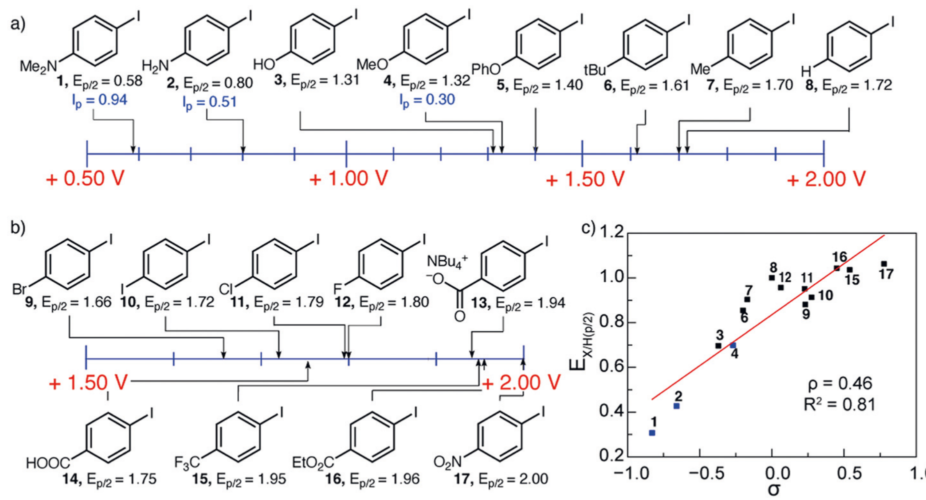

Figure 1 Summary of electrochemical data for 4-substituted aryl iodides with a) electron-donating and b) electron-withdrawing substituents. I_p values are reported for all quasireversible substrates. c) Hammett analysis provided from $E_{x/H(p/2)}$ versus the substituent constant (σ). Blue squares indicate quasireversibility and black squares indicate irreversible CVs.

Differently substituted aryl iodides show disparate electrochemical behavior, from fully reversible to fully irreversible one-electron oxidation. To obtain detailed understanding of the relationship between structure and electrochemical activity, despite the differences in electrochemical reversibility, we have used the method of half-peak potentials ($E_{p/2}$). In general, we observe linear free energy relationships for the $E_{p/2}$ of substituted aryl iodides. These linear relationships include both substrates that display reversible and irreversible oxidation waves by CV analysis, which suggests that the measured $E_{p/2}$ are well-correlated with the thermodynamic potential for one-electron oxidation.

This method was chosen as a result of the inability to measure a reductive peak potential (E_{pc}) for irreversible systems, which prevents direct experimental determination of $E_{1/2}$, and because simple reporting of the peak oxidative potential (E_{pa}) traditionally overestimates thermodynamic potentials.[19] Practically, $E_{p/2}$ was calculated by finding the potential at half of the baseline-corrected peak oxidative current (I_{pa}).[19] Quasireversible and reversible redox events were further evaluated by the peak current ratio ($I_{pc}/I_{pa} = I_p$), which is a parameter that describes the extent of reversibility of the redox process. $E_{p/2}$ values are presented for all aryl iodides and I_p values (in blue in the figures) are presented only for those aryl iodides that display quasireversible electrochemistry. In all cases, cyclic voltammograms (CVs) were measured by using 0.1 M $[TBA]PF_6$ solutions in hfip with 5 mM of the relevant analyte at 0.1 V/s and were referenced to Fc^+/Fc (TBA: tetrabutylammonium; hfip: 1,1,1,3,3,3-hexafluoroisopropanol; Figure S1–S70 in the Supporting Information). All of the reported electrochemical experiments are carried out in hfip owing to the ubiquity of this solvent in reported electrochemical systems.[20]

Electrochemical Properties of 4-Substituted Aryl Iodides

We began our studies by investigating the effect of 4-substitution on the electrochemistry of aryl iodides (Figure 1). These studies indicated a predictable relationship between the donicity of the *para* substituent and the resultant potential for one-electron oxidation: electron-donating groups (Figure 1a) lower the $E_{p/2}$ and electron-withdrawing groups (Figure 1b) increase the $E_{p/2}$.[21] The Hammett plot, generated by plotting the half-peak potential of variously 4-substituted aryl iodides ($E_{x(p/2)}$) normalized by the half-peak potential of iodobenzene ($E_{H(p/2)}$) versus the substituent constant (σ), is linear with ρ = 0.46 (Figure 1c). The electrochemical reversibility of the substrates included in this plot, evaluated by the ratio of I_{pc}/I_{pa}, varies significantly (**1**, **2**, and **4** display various degrees of reversible one-electron oxidation [I_p = 0.94, 0.51, and 0.30, respectively], whereas **3** and **5–17** display irreversible oxidation [I_p = 0.00]). The linearity of the Hammett plot, despite these differences in reversibility for the constituent species, suggests that the electron-transfer kinetics are similar across this family of substituted aryl iodides.

Electrochemical Properties of 3- and 2-Substituted Aryl Iodides

An analogous set of data was obtained for 3-substituted aryl iodides (see the Supporting Information, Section D). The $E_{p/2}$ values measured for these systems were less sensitive to the identity of the substituent (ρ = 0.24 (R^2 = 0.41); see Section D.2 in the Supporting Information for the Ham-

Downloaded by: Texas A&M University. Copyrighted material.

mett plot), and the CVs were uniformly irreversible regardless of the functional group (see the Supporting Information, Section D.1).

We next evaluated 2-substituted aryl iodides (Figure 2), both simple 2-substituted structures (**18**–**26**), and structures in which the 2-substituent can participate in five-membered chelates via coordination to the oxidized iodine center (**27**–**34**). The Taft plot, generated by plotting the half-peak potential of simple 2-substituted aryl iodides ($E_{x(p/2)}$) normalized by the half-peak potential of iodobenzene ($E_{H(p/2)}$) versus the polar substituent constant (σ^*),[22] is linear with ρ = 0.26 (Figure 2c). In general, data obtained from CV analysis of compounds with *ortho* substituents display a similar trend in $E_{p/2}$ values to that observed with *para*-substituted compounds: electron-donating substituents suppress the potential needed for oxidation, whereas electron-withdrawing substituents increase the potential required. The CVs of electron-rich substrates in which the 4-substituent features a non-bonding pair of electrons, that is, **1** (4-*N*,*N*-dimethylamino), **2** (4-amino), **4** (4-methoxy), **9** (4-bromo), and **12** (4-fluoro), display $E_{p/2}$ values lower than the corresponding 2-substituted derivatives, that is, **19** (2-*N*,*N*-dimethylamino), **20** (2-amino), **21** (2-methoxy), **25** (2-bromo), and **26** (2-fluoro).[23] These observations are consistent with a combination of resonance and inductive effects: both 4- and 2-substituents are resonance donors but inductive effects are more significant for 2-substituents than for the corresponding 4-substituents. Despite the similar trends in the $E_{p/2}$ values, stark differences in reversibility were noted for 4- versus 2-substituted aryl iodides: in contrast to the reversible CVs for **1** (4-*N*,*N*-dimethylamino), **2** (4-amino), and **4** (4-methoxy), reversibility was severely diminished or lost entirely for the corresponding *ortho* derivatives **19** (2-*N*,*N*-dimethylamino), **20** (2-amino), and **21** (2-methoxy).

The differences in $E_{p/2}$ between 4- and 2-substituted aryl iodides with potentially chelating substituents provide insight into the potential stabilization of the anodically generated iodanyl radicals by intramolecular coordination. The CVs of compounds **27** (2-carboxylate), **29** (2-ethyl benzoate), and **30** (2-nitro) provided $E_{p/2}$ values that were 80–160 mV lower in potential than those of the *para*-substituted counterparts **13** (4-carboxylate), **16** (4-ethyl benzoate), and **17** (4-nitro), likely as a result of stabilizing chelation of the substituent to the incipient iodanyl radical. In the case of redox-active functional groups, such as 2-iodobenzoate (**27**), a second irreversible oxidation event is observed at $E_{p/2}$ = 1.42 V vs. Fc^+/Fc, in addition to the $E_{p/2}$ = 1.71 V vs. Fc^+/Fc that we attribute to aryl iodide oxidation; we hypothesize that this additional feature arises from direct oxidation of the carboxylate functional group (Figure S27). A second oxidation event is also observed for 4-iodobenzoate (**13**) at $E_{p/2}$ = 1.70 V vs. Fc^+/Fc, 280 mV higher than that for **27** (Figure S13). The additional oxidative features observed for **13** and **27** are not observed for the carboxylic acid or ethyl benzoate substituted aryl iodides **28** and **29**, respectively (Figure S28 and S29).

Electrochemical Properties of 2-Substituted 4-Iodoanisole Derivatives

Based on the ubiquity of 4-iodoanisole as a mediator in hypervalent iodine electrocatalysis and electrochemistry, we focused specific attention on the impact of substitution on this scaffold. Figure 3 summarizes the electrochemical data collected for a family of 2-substituted 4-iodoanisole

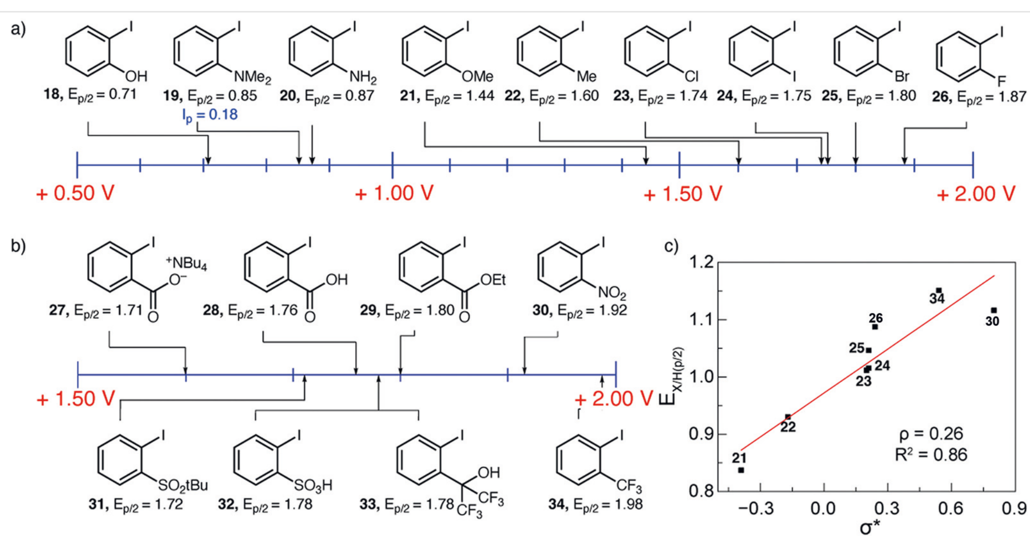

Figure 2 Summary of electrochemical data for 2-substituted aryl iodides with a) simple functional groups and b) potentially coordinating Lewis basic substituents. I_p values are not given for irreversible systems. c) Taft plot analysis provided from $E_{x/H(p/2)}$ versus the polar substituent constant (σ). Black squares indicate irreversible CVs.

Downloaded by: Texas A&M University. Copyrighted material.

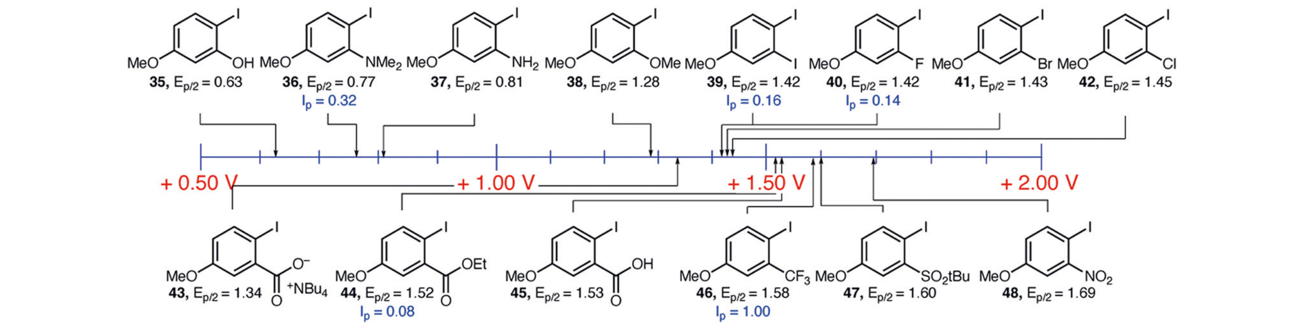

Figure 3 Summary of electrochemical data for 2-substituted 4-iodoanisole derivatives. I_p values are not given for irreversible systems.

derivatives. Similar to the trends observed for 2-substituted aryl iodides above, electron-rich substrates bearing 2-hydroxy (**35**), 2-*N*,*N*-dimethylamino (**36**), or 2-amino (**37**) substituents in the *ortho* position display lower $E_{p/2}$ values than that of **4**; however, these derivatives feature decreased electrochemical reversibility relative to that of **4**. Electron-deficient substrates, such as those bearing 2-iodo (**39**), 2-fluoro (**40**), 2-bromo (**41**), 2-chloro (**42**), 2-ethyl benzoate (**44**), 2-carboxy (**45**), 2-trifluoromethyl (**46**), 2-*tert*-butylsulfonyl (**47**), and 2-nitro (**48**), display increased $E_{p/2}$ values on comparison with that of 4-iodoaniosle (**4**); however, in contrast to the aforementioned electron-rich iodoanisole derivatives, they retain varying degrees of reversibility. In general, the presence of a *para*-methoxy substituent in compounds **36**, **39**, **40**, **44**, and **46** results in increased reversibility relative to that of the corresponding compounds without this substituent, that is, **18**, **24**, **33**, **28**, and **34**, respectively. Surprisingly, despite trifluoromethyl being electron withdrawing, the CV of **46** showed a 400 mV decrease in $E_{p/2}$ in comparison with that of **34**, as well as complete electrochemical reversibility (I_p = 1.00). We hypothesize that the observed electrochemical behavior of **46** is a result of stabilization from a pseudocyclic five-membered chelate with one of the C–F bonds to the iodine-centered radical cation. Other *ortho* Lewis bases such as the carboxylate (**43**), carboxylic acid (**45**), *tert*-butylsulfone (**47**), and nitro (**48**) provide irreversible CVs. *ortho*-Halogenated compounds such as the bromide (**41**) and chloride (**42**) display irreversible anodic features, in contrast to **39** and **40**, likely as a result of poor orbital overlap with the neighboring iodine.

Electrochemical Properties of Dimethoxy Iodobenzene Derivatives

Based on the recent demonstration that diiodoveratrole (**51**) is an efficient electrocatalyst for C–H/E–H coupling via an isolable iodanyl radical,[18] we examined the electrochemical properties of a family of dimethoxy iodobenzene derivatives (Figure 4). In general, this family of compounds displays enhanced electrochemical reversibility relative to the values for the anisole derivatives summarized in Figure 3. In particular, despite *ortho*-bromo (**41**), *ortho*-carboxylic acid (**45**), and *ortho*-*tert*-butylsulfonyl (**47**) substitution producing irreversible CVs in the monomethoxy aryl iodides, similar substitutions with the veratrole moiety, that is, compounds **53**, **57**, and **59**, provided quasireversible CVs with I_p = 0.70, 0.53 and 0.90, respectively. Compounds with *ortho*-iodo (**51**), *ortho*-fluoro (**52**), and *ortho*-ethyl benzoate (**56**) substitutions showed significantly increased reversibility (I_p = 0.94, 0.98, and 1.03, respectively) relative to that of the corresponding monomethoxy derivatives **39**, **40**, and **44** (I_p = 0.16, 0.14, and 0.08, respectively). Notably, the *ortho*-fluorinated compound **52** displayed the same reduction po-

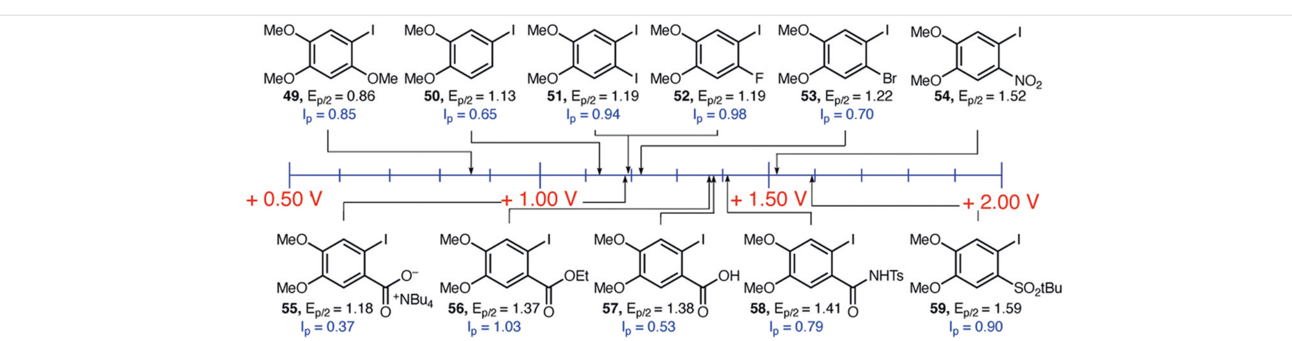

Figure 4 Summary of electrochemical data for iodoveratrole derivatives. I_p values are not given for irreversible systems.

Downloaded by: Texas A&M University. Copyrighted material.

tential ($E_{p/2}$ = 1.19 V) as the *ortho*-iodinated compound **51** ($E_{p/2}$ = 1.19 V), which is in contrast to the trend observed in Figure 2 between compounds **26** ($E_{p/2}$ = 1.87 V) and **24** ($E_{p/2}$ = 1.75). The CV of 3,4-dimethoxyiodobenzene (**50**) results in two redox waves, at 1.13 V vs. Fc^+/Fc (I_p = 0.65) and 1.36 V vs. Fc^+/Fc (I_p = 0.06, Figure S50). Lastly, in contrast to the irreversible CV with the *ortho*-methoxy substituent in the anisole derivative (**38**), the CV of the trimethoxy-substituted aryl iodide **49** displays moderate electrochemical reversibility, I_p = 0.85, and a decreased $E_{p/2}$ of 0.86 V vs. Fc^+/Fc.

Electrochemical Properties of Miscellaneous Additional Aryl Iodides

Figure 5 summarizes the electrochemical behavior of additional electron-rich aryl iodides, as well as that of biaryl structures that have found application in hypervalent iodine catalysis with peracids, not anodes, as the terminal oxidant.

In the context of electron-rich substrates, *para*-substituted diiododimethoxyarene **60** shows a decreased reduction potential ($E_{p/2}$ = 1.09 V vs. Fc^+/Fc) and a similar reversibility (I_p = 0.93) to those of **51** ($E_{p/2}$ = 1.19 V vs. Fc^+/Fc, I_p = 0.94). The dioxole moiety in compound **61** results in a slightly decreased electrochemical reversibility (I_p = 0.87) relative to that of **51** (I_p = 0.94). 1,2-Diiodo-4,5-dimethylbenzene (**68**) displayed a higher reduction potential ($E_{p/2}$ = 1.58 V vs. Fc^+/Fc) than that of **51** ($E_{p/2}$ = 1.19 V vs. Fc^+/Fc) and with no observed electrochemical reversibility, proving the importance of resonance from the methoxy substituents. In the context of biaryldiiodides, compounds **63** and **64** both display improved reversibility (I_p = 0.70 and 0.35, respectively) relative to that of the monoaryl counterparts, **50** and **62** (I_p = 0.65 and 0.00, respectively). Both methoxy-substituted biaryldiiodides **63** and **64** show improved reversibility over that of the irreversible parent Kita catalyst **65**.[24] Compound **63** displays two disparate reversible redox waves, and overlaps with monomer **50**, one at 1.13 V vs. Fc^+/Fc (I_p = 0.70) and one at 1.36 V vs. Fc^+/Fc (I_p = 0.93, Figure S63). A general trend can be drawn that the overall arene reduction potential decreases and electrochemical reversibility increases with an increase of methoxy substituents. Similarly, *ortho*-iodo and *ortho*-Lewis basic groups generally show improved electrochemical reversibility.

Decomposition of Anodically Generated Iodanyl Radicals

The application of aryl iodides in electrocatalysis is often plagued by high catalyst loading, which we hypothesize arises from the instability of anodically generated intermediates. Consistent with this hypothesis, the survey of anodic aryl iodide chemistry above often resulted in the observation of electrochemically irreversible processes or complex cyclic voltammograms. To evaluate the origins of the observed electrochemical irreversibility and to evaluate potential decomposition pathways, we pursued a detailed study of the chemistry of iodanyl radicals derived from 4-iodoanisole (**4**) and 3,4-dimethoxyiodobenzene (**50**), which both present complicated quasireversible CVs (Figure 6).

4-Iodoanisole (**4**) is a competent electrocatalyst for C–H/N–H coupling[17] and *gem*-difluorination of dithioketals;[6,10] however, its application in catalysis typically requires 25 mol% catalyst loading (or higher). The CV of **4** in hfip displays a shoulder with a peak potential (E_{pa}) at 1.39 V vs. Fc^+/Fc (Figure 6a). Increasing the scan rate for the CV of **4** results in the disappearance of the shoulder. We hypothesized that the increased reversibility may be a resut of reduction of the incipient iodanyl radical outcompeting chemical degradation at higher scan rates (Figure S71a). To evaluate this hypothesis, we carried out chemical oxidation of a CH_2Cl_2 solution of **4** with (bis(trifluoroacetoxy)io-

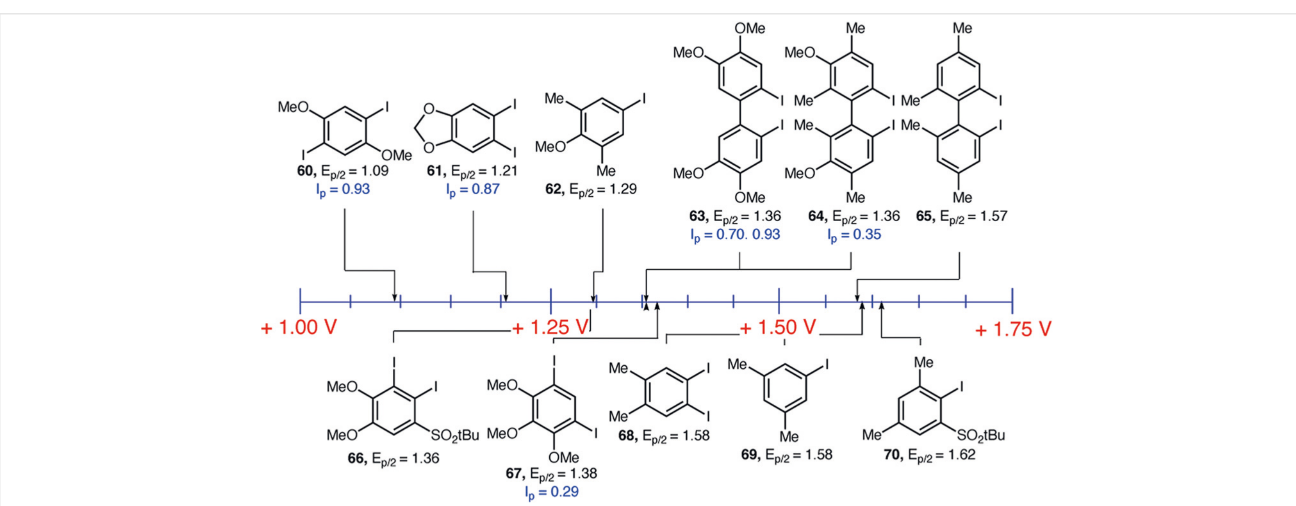

Figure 5 Summary of electrochemical data for additional electron-rich aryl iodides.

Downloaded by: Texas A&M University. Copyrighted material.

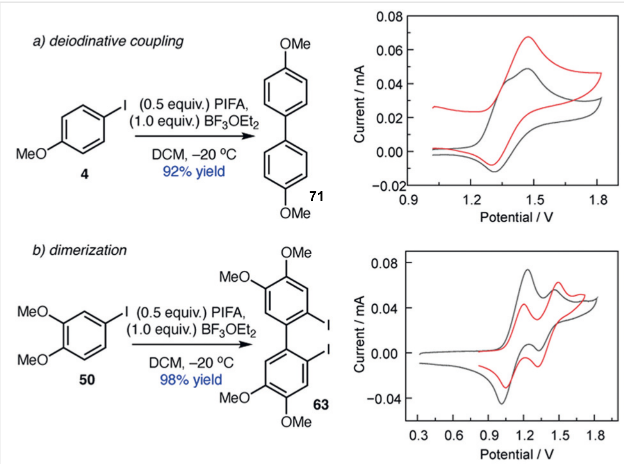

Figure 6 a) Deiiodinative coupling via chemical oxidation of 4-iodoanisole (**4**, black line) to 4,4′-dimethoxy-1,1′-biphenyl (**71**, red line) and b) dimerization of 3,4-dimethoxyiodobenzene (**50**, black line) to 2,2′-diiodo-4,4′,5,5′-tetramethoxy-1,1′-biphenyl (**63**, red line) with the corresponding CV analysis.

do)benzene (PIFA, 0.5 equiv) and $BF_3{\cdot}OEt_2$, conditions that were previously developed for the synthesis of iodanyl radicals.[18] Combination of these reagents resulted in initial formation of a dark blue solution, presumably **4⁺**; upon warming, spectral bleaching occurred and ^1H NMR analysis of the resulting solution indicated the deiodinated dimer **71** in 92% yield. Independent analysis of the CV of biaryl compound **71** indicated the presence of a feature at E_{pa} = 1.49 V vs. Fc^+/Fc, which overlaps with the peak observed in the CV of **4** and suggests that deiodinative coupling is operative on the timescale of the CV; the shoulder in the CV of **4** arises from in situ formation of **71**. Importantly, electrolysis of **4** in the presence of [TMA]OAc, conditions necessary for catalytic C–H/N–H coupling, does not result in the formation of biaryl **71** (and the shoulder is not observed in the square-wave voltammetry results for this mixture; Figure S71b,c). These observations indicate that, although decomposition of **4⁺** to **71** is viable, reaction conditions can be optimized to avoid this decomposition pathway and it is not observed under catalytic conditions.

The electrochemistry of **50** demonstrates a different potential dimerization pathway available to iodanyl radicals. The CV of **50** displays two oxidation events with significantly different amplitude. Similar chemical oxidation of a CH_2Cl_2 solution of **50** with PIFA (0.5 equiv) and $BF_3{\cdot}OEt_2$ resulted in the initial formation of a purple solution, and ^1H NMR analysis following spectral bleaching showed 98% homocoupled product **63** (Figure 6b). The CV of independently prepared **63** displays two oxidation events with similar amplitudes, as would be expected for two one-electron oxidation processes. The lower-potential features in the CVs of **50** and **63** are overlapping; the disparity in intensities observed in the CV of **50** is likely owing to partial conversion into **63** on the timescale of the CV experiment. Consistent with this hypothesis, increasing the CV scan rate of **50** results in a decrease in the peak at E_{pa} = 1.49 V vs. Fc^+/Fc, indicating that this peak is likely the result of a rapid chemical reaction following the first oxidation (Figure S72). The nucleophilicity of **50** and vacant electrophilic *ortho* site of the oxidized radical cation **50⁺** apparently renders this iodanyl radical susceptible to rapid dimerization.

In conclusion, we have provided a broad survey of the electrochemical properties of aryl iodides. Despite the significant differences in electrochemical reversibility across this family of compounds, the potential required for one-electron oxidation of these compounds obeys standard free-energy relationships. These observations suggest that the observed onset potentials are a useful proxy for the thermodynamics of oxidation and may be a simple tool for optimization of aryl iodide catalysts. In addition, we have described two potential decomposition pathways for iodanyl radicals in which dimerization, either with or without concurrent deiodination, results in consumption of the initial aryl iodide. We anticipate that the combination of electrochemical data and well-described decomposition mechanisms will be useful in guiding the continued development of aryl iodides as metal-free electrocatalysts.

Conflict of Interest

The authors declare no conflict of interest.

Funding Information

The authors thank the Welch Foundation (A-1907) and the National Science Foundation (CAREER 1848135) for financial support.

Supporting Information

Supporting information for this article is available online at https://doi.org/10.1055/a-2029-0617.

References

(1) Frey, B.; Maity, A.; Tan, H.; Roychowdhury, P.; Powers, D. C. *Iodine Catalysis in Organic Synthesis*; Wiley-VCH: Weinheim, **2022**, 335.
(2) Miller, L. L.; Hoffmann, A. K. *J. Am. Chem. Soc.* **1967**, *89*, 593.
(3) Singh, F. V.; Shetgaonkar, S. E.; Krishnan, M.; Wirth, T. *Chem. Soc. Rev.* **2022**, *51*, 8102.
(4) Yoshimura, A.; Zhdankin, V. V. *Chem. Rev.* **2016**, *116*, 3328.
(5) Zhdankin, V. V. *Hypervalent Iodine Chemistry: Preparation, Structure and Synthetic Applications of Polyvalent Iodine Compounds*; John Wiley & Sons: Chichester, **2014**.
(6) Fuchigami, T.; Fujita, T. *J. Org. Chem.* **1994**, *59*, 7190.
(7) Kong, X.; Lin, L.; Chen, X.; Chen, Y.; Wang, W.; Xu, B. *ChemSusChem* **2021**, *14*, 3277.
(8) Massignan, L.; Tan, X.; Meyer, T. H.; Kuniyil, R.; Messinis, A. M.; Ackermann, L. *Angew. Chem. Int. Ed.* **2020**, *59*, 3184.

Downloaded by: Texas A&M University. Copyrighted material.

(9) Paveliev, S. A.; Segida, O. O.; Bityukov, O. V.; Tang, H.-T.; Pan, Y.-M.; Nikishin, G. I.; Terent'ev, A. O. *Adv. Synth. Catal.* **2022**, *364*, 3910.
(10) Hara, S.; Hatakeyama, T.; Chen, S.-Q.; Ishi-i, K.; Yoshida, M.; Sawaguchi, M.; Fukuhara, T.; Yoneda, N. *J. Fluorine Chem.* **1998**, *87*, 189.
(11) Broese, T.; Francke, R. *Org. Lett.* **2016**, *18*, 5896.
(12) Elsherbini, M.; Winterson, B.; Alharbi, H.; Folgueiras-Amador, A. A.; Génot, C.; Wirth, T. *Angew. Chem. Int. Ed.* **2019**, *58*, 9811.
(13) Elsherbini, M.; Wirth, T. *Chem. Eur. J.* **2018**, *24*, 13399.
(14) Koleda, O.; Broese, T.; Noetzel, J.; Roemelt, M.; Suna, E.; Francke, R. *J. Org. Chem.* **2017**, *82*, 11669.
(15) Sawamura, T.; Kuribayashi, S.; Inagi, S.; Fuchigami, T. *Adv. Synth. Catal.* **2010**, *352*, 2757.
(16) Wirth, T. *Curr. Opin. Electrochem.* **2021**, *28*, 100701.
(17) Maity, A.; Frey, B. L.; Hoskinson, N. D.; Powers, D. C. *J. Am. Chem. Soc.* **2020**, *142*, 4990.
(18) Frey, B. L.; Figgins, M. T.; Van Trieste, G. P. III.; Carmieli, R.; Powers, D. C. *J. Am. Chem. Soc.* **2022**, *144*, 13913.
(19) Roth, H. G.; Romero, N. A.; Nicewicz, D. N. *Synlett* **2016**, *27*, 714.
(20) Ramos-Villaseñor, J.; Rodríguez-Cárdenas, E.; Díaz, C.; Frontana-Uribe, B. *J. Electrochem. Soc.* **2020**, *167*, 155509.
(21) Shikata, M. T. *Collect. Czech. Chem. Commun.* **1938**, *10*, 368.
(22) Lin, G.; Liu, Y. C.; Lin, Y. F.; Wu, Y. G. *J. Enzyme Inhib. Med. Chem.* **2004**, *19*, 395.
(23) The CV of **18** (2-phenol) is significantly broader than the CV of **3** (4-phenol), which makes it difficult to directly compare the $E_{p/2}$ values.
(24) Ito, M.; Kubo, H.; Itani, I.; Morimoto, K.; Dohi, T.; Kita, Y. *J. Am. Chem. Soc.* **2013**, *135*, 14078.

Downloaded by: Texas A&M University. Copyrighted material.